ORCA – Online Research @ Cardiff

This is an Open Access document downloaded from ORCA, Cardiff University's institutional repository:https://orca.cardiff.ac.uk/id/eprint/117765/

This is the author's version of a work that was submitted to / accepted for publication.

Citation for final published version:

Dhara, Soumen , Niang, Kham M., Flewitt, Andrew J., Nathan, Arokia and Lynch, Stephen A. 2019. Photoconductive laser spectroscopy as a method to enhance defect spectral signatures in amorphous oxide semiconductor thin- film transistors. Applied Physics Letters 114 (1) , 011907. 10.1063/1.5070141

Publishers page: https://doi.org/10.1063/1.5070141

Please note:
Changes made as a result of publishing processes such as copy-editing, formatting and page numbers may not be reflected in this version. For the definitive version of this publication, please refer to the published source. You are advised to consult the publisher's version if you wish to cite this paper.

This version is being made available in accordance with publisher policies. See http://orca.cf.ac.uk/policies.html for usage policies. Copyright and moral rights for publications made available in ORCA are retained by the copyright holders.

Photoconductive Laser Spectroscopy as a Method to Enhance Defect Spectral Signatures in Amorphous Oxide Semiconductor Thin-film Transistors

Soumen Dhara,[1, a)] Kham M. Niang,[2] Andrew J. Flewitt,[2] Arokia Nathan,[2] and Stephen A. Lynch[1, b)]
[1)] *School of Physics and Astronomy, Cardiff University, Cardiff CF24 3AA, United Kingdom.*
[2)] *Electrical Engineering Division, University of Cambridge, Cambridge CB3 0FA, United Kingdom.*

(Dated: 19 October 2018)

SUPPLEMENTARY MATERIAL

Figure S1 shows the layer structure and footprint of the TFTs. Bottom gate, inverted staggered structure TFTs

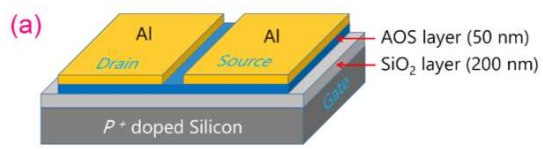

FIG. S1. A schematic diagram of showing the later structure and footprint of TFT made with the active AOS layer.

were fabricated using thermally grown SiO_2 films (thickness ∼200 nm) on heavily doped p-type Si (100) substrates ($\rho = 0.01 - 0.02$ Ωcm), which are used as the gate dielectric and gate electrode, respectively. Both ZTO and IGZO thin-films were amorphous (a-ZTO and a-IGZO), whereas the ZnO thin-films were nano-crystalline. The thin films were deposited by sputtering to a thickness of ∼50 nm. A post deposition anneal in air was performed at 200 °C for a-ZTO and at 500°C for the ZnO and a-IGZO thin-films. Top ohmic contacts for the source and drain were formed by thermal evaporation of aluminium.

Figure S2 shows a schematic of experimental setup. The illumination is provided by an EKSPLA PL2251B-PG411 wavelength tunable picosecond laser system. The

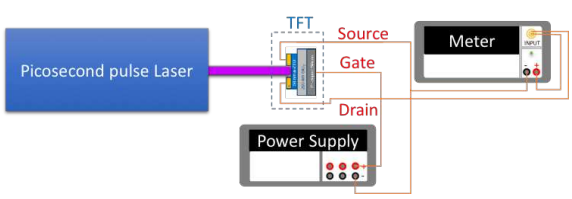

FIG. S2. A schematic diagram of the experimental setup of the photoexcited current spectroscopy. The active semiconductor area of the TFT was perpendicularly illuminated with a ps-pulsed laser beam. The corresponding photogenerated drain-to-source current (I_{phot}) was measured using a Keithley meter. A Labview program was used to automate the measurement.

[a)] Electronic mail: soumen5484@yahoo.co.in
[b)] Electronic mail: LynchSA@cardiff.ac.uk

EKSPLA system combines a picosecond Nd:YAG optical pump at 1064 nm which is used to generate the 2nd and 3rd harmonic beams at 532 nm and 355 nm. The wavelength tuning is provided by mixing the harmonics in an optical parametric oscillator (OPO), to give signal (410 - 709 nm) and idler (710 - 2300 nm) idler beams. A further extension of the tuning range into the UV band (210 - 409) nm was achieved through second harmonic generation. The active semiconductor area of the TFT was illuminated (perpendicular to the plane of the thin film) with a pulsed picosecond laser beam (temporal pulsewidth ∼30 ps and repetition frequency 20 Hz). During the measurement, the wavelength of the laser signal was varied from 1000 → 300 nm in 2 nm steps (always starting from the longer wavelength side) and the corresponding photogenerated drain-to-source current (I_{phot}) was measured using a Keithley meter (Model-6517B) with integration time of 20 sec. A Labview program was used to automate the measurement.

Figure S3 shows the pulse energy (in μJ) as a function wavelength for the picosecond-pulsed laser measured in the spectral range of 4.13 - 1.24 eV (300 - 1000 nm). This figure shows that the laser emission is not contin-

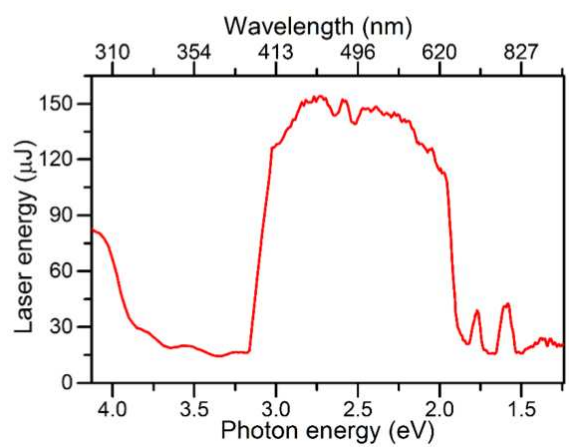

FIG. S3. Pulse energy (in μJ) as a function wavelength for the picosecond-pulsed laser measured in the spectral range of 4.13 - 1.24 eV (300 - 1000 nm).

uously tunable across the full wavelength change, which is due to the optical generation mechanism. The most intense laser pulses are derived directly from the OPO signal 410 - 709 nm. Above 710 nm the lower energy idler beam is used. Below 410 nm, the UV wavelength

tunable beam is generated through 2nd harmonic generation of a portion of the signal beam. The variation in pulse energies for the three regions is normalised as described in the main text of the paper.

Figure S4 shows the X-ray photoelectron spectroscopy binding energy spectrum for the O1s core level of the a-ZTO thinfilm. The individual component (O^{2-} and

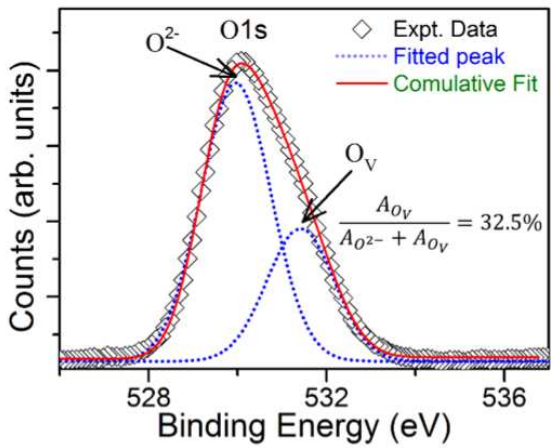

FIG. S4. X-ray photoelectron spectroscopy binding energy spectrum for the O1s core level of the a-ZTO thinfilm.

O_V) in the broad and asymmetric O1s spectrum is identified after fitting with multiple Gaussian peaks. The solid red line represents the combined fitting of the sum of all the individual components (blue dotted lines). The peak centered at 530.0 eV represents oxygen ions connected with metal ions known as the lattice oxygen, O^{2-}. The higher binding energy peak (O_V) centered at 531.4 eV is associated with oxygen ions that are in oxygen deficient regions within the matrix of a-ZTO (oxygen vacancy states). The relative oxygen vacancy content estimated from the integrated peak area of O^{2-} and O_V peaks is found to be 32.5%.

Figure S5 shows the transistor characteristic data of the ZnO and a-IGZO TFTs from which the transfer characteristics were derived. For the ZnO TFTs, the transfer characteristics were, $V_{FB} = -17.0$ V, $V_{Th} = 0.8$ V, and $\mu_{FE} = 3.5$ cm^2/Vs. For the a-IGZO TFTs, the transfer characteristics were, $V_{FB} = -6.0$ V, $V_{Th} = 7.7$ V, and $\mu_{FE} = 9.95$ cm^2/Vs.

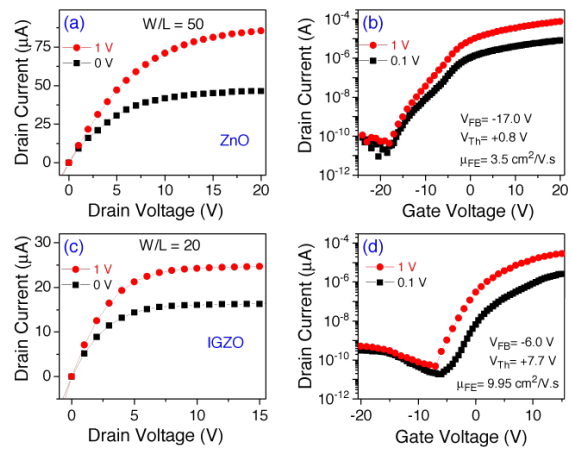

FIG. S5. The transistor characteristic data of the ZnO and a-IGZO TFTs, (a) and (c) output characteristics, and (b) and (d) transfer characteristics. The W/L ratio of the active semiconductor channel was fixed to 50 for the ZnO TFT and 20 for the a-IGZO TFT.